Voltage and Current Sources for Massive Conductors Suitable With the A-χ Geometric Eddy-Current Formulation

Paweł Dłotko[1], Ruben Specogna[2], and Francesco Trevisan[2]

[1]Jagiellonian University, Institute of Computer Science, Kraków 31-007, Poland
[2]Dipartimento di Ingegneria Elettrica, Gestionale e Meccanica (DIEGM), Università di Udine, Udine 33100, Italy

The aim of the paper is to present an automatic and general technique, suitable with the A-χ geometric eddy-current formulation, to impose sources over massive conductors of any shape. For this purpose, the *localized source approach* is used, which does not require the solutions of steady-state conduction problems in the preprocessing stage. Nevertheless, this approach needs a *thick cut* in each active conductor, which is usually found "by hand." In this paper, an automatic and general algorithm to compute such thick cuts is introduced. Some benchmark problems are presented to demonstrate the generality and the robustness of the algorithm.

***Index Terms*—Cell method, cohomology computation, current and voltage sources, discrete geometric approach (DGA), eddy-currents, finite integration technique (FIT), thick cuts.**

I. Introduction

THE so-called "discrete geometric approach" (DGA) [1], similar to the finite integration technique (FIT) [2] or the cell method [3], allows to solve directly Maxwell's equations in an alternative way with respect to the classical finite elements.

In this paper, an automatic technique to enforce sources on massive conductors, suitable with the eddy-current A-χ geometric formulation [4], is introduced. In particular, the *localized source approach* [5], [6] is considered. This approach presents many advantages with respect to the *distributed source approach* [6]; For example, it does not require steady-state conduction problem solutions in the preprocessing stage. Furthermore, the localized source approach is based on global quantities—voltages and currents—which enables a straightforward coupling between the eddy-current formulation and electric circuits.

The domain of interest D of the eddy-current problem, which is a subset of the three-dimensional Euclidean space $\mathbb{R}^3$, has been partitioned into an active conductive region D_s, a passive conductive region D_c, and a nonconductive region D_a. We assume that the region D_s—where sources are enforced—consists of the union of N disjoint conductors $D_s^j, j = \{1, \ldots, N\}$, such that $D_s = \bigcup_{j=1}^{N} D_s^j$. Moreover, we assume that the first Betti number [7] of each domain $D_s^j, j = \{1, \ldots, N\}$, is one.[1]

No assumption is given about the conductors belonging to D_c.

The domain D is covered by a tetrahedral finite element mesh. The corresponding simplicial complex $\mathcal{K}$ (see [3]) is referred to as primal complex. From the primal simplicial complex, the barycentric dual complex $\mathcal{B}$ is also introduced [3]. The incidence matrix between edges e and nodes n of the primal complex $\mathcal{K}$ is denoted by $\mathbf{G}$, by $\mathbf{C}$ is denoted the incidence matrix between faces f and edges e of $\mathcal{K}$, and by $\mathbf{D}$ the incidence matrix between tetrahedra v and faces f of $\mathcal{K}$. The matrices $\tilde{\mathbf{G}} = \mathbf{D}^T$, $\tilde{\mathbf{C}} = \mathbf{C}^T$, and $\tilde{\mathbf{D}} = -\mathbf{G}^T$ describe the corresponding incidence matrices of the dual barycentric complex $\mathcal{B}$ [3].

The localized source approach needs a *thick cut* [6] for each active conductor, which is usually found "by hand" [5]. When dealing with complicated geometries or a big number of active conductors, an automatic technique to find such thick cuts can be very useful. This is the reason why we propose in Section V an original, general, and completely automatic topology-based algorithm to construct thick cuts, which does not require any prior knowledge about the geometry of the active conductors.

II. Thick Cuts for the Tori

Let us consider each active conductor D_s^j, with $j \in \{1, \ldots, N\}$. The elements of $\mathcal{K}$ and $\mathcal{B}$ that correspond to geometrical entities belonging to D_s^j, are denoted as $\mathcal{K}_s^j$ and $\mathcal{B}_s^j$, respectively.

For each edge e belonging to $\mathcal{K}_s^j$, an integer is specified. The values are determined in such a way that the sum (with incidence) of the values of the edges belonging to a cycle is equal to n (or $-n$) if and only if the cycle "goes n times around the conductor, on or inside it" (All homologically trivial cycles [7] go around the conductor zero times. Moreover, since we focus on solid toric regions only, the cycles that goes around the branch of each conductor are homologically trivial.).[2]

The integer values relative to each edge $e \in D_s^j$ are stored into arrays $(\mathbf{c}^j)_e, j = \{1, \ldots, N\}$, one array for each conductor. The array $\mathbf{c}^j$ is a *thick cut*. More precisely, the thick cut is the representative of a first cohomology group $H^1(\mathcal{K}_s^j)$ [7] generator.

On the left of Fig. 1, an example of torus-like active conductor is considered. On the right of Fig. 1, the black edges represent the edges whose integer coefficients in the thick-cut array are nonzero.

Manuscript received December 17, 2009; accepted February 10, 2010. Current version published July 21, 2010. Corresponding author: R. Specogna (e-mail: ruben.specogna@uniud.it).

Color versions of one or more of the figures in this paper are available online at http://ieeexplore.ieee.org.

Digital Object Identifier 10.1109/TMAG.2010.2043510

[1]This assumption is not restrictive in practice since sources are usually imposed only on torus-like conductors. This assumption allows to consider knotted active conductors. In case the user needs to relax this assumption, it is still possible to directly apply the general algorithm described in Section V-B5.

[2]Formally speaking, since the first homology group $H_1(\mathcal{K}_s^j) = \mathbb{Z}$ [7], then there exists one generator $[g]$ of $H_1(\mathcal{K}_s^j)$. For a given cycle c, the sum of $(\mathbf{c})_e^j$ with incidence is equal $n \in \mathbb{Z}$ if $c \in [ng]$, where $[ng]$ indicates the homology class of the cycle ng. In the considered case, the homology group is torsion-free [7], and there is a direct correspondence between first homology and cohomology generators.

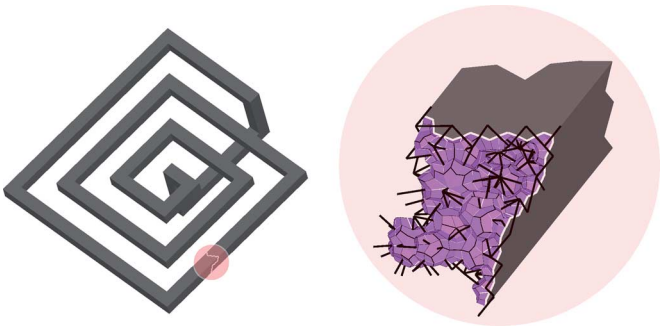

Fig. 1. (left) Example of torus-like conductor. (right) Zoom on a portion of the conductor in the neighborhood of the nonzero-valued edges in the thick cut (the thick black edges). The collection of dual faces, dual to nonzero-valued thick-cut edges, form a surface S^j on the dual complex that "cuts" the conductor.

Considering the union of dual faces one-to-one with nonzero-valued thick-cut edges, a surface S^j that "cuts" the conductor is obtained on the dual complex;[3] see, for example, on the right in Fig. 1. The reader should be aware that the surface S^j is always orientable, but, in general, can be also self-intersecting.

III. Localized Voltage Sources

The localized voltage source approach [6], also referred to as "generalized source potential" in [5], is now recalled. Let us define the array $\mathbf{U}_s$ as

$$(\mathbf{U}_s)_e = \sum_{j=1}^{N} U^j_{\rm tot}(\mathbf{c}^j)_e \quad \forall\, e \in D_s \tag{1}$$

where $U^j_{\rm tot}$ is the enforced voltage on the jth conductor. Note that, for a fixed edge e, only one term of the sum is nonzero. Then, the A-χ formulated eddy-current problem in the frequency domain becomes [6]

$$\begin{array}{ll}
(\mathbf{C}^T\boldsymbol{\nu}\mathbf{C}\mathbf{A})_e = 0 & e \in D_a \\
(\mathbf{C}^T\boldsymbol{\nu}\mathbf{C}\mathbf{A})_e + i\omega(\boldsymbol{\sigma}_s\mathbf{A}_s + \boldsymbol{\sigma}_s\mathbf{G}_s\boldsymbol{\chi}_s)_e = (\mathbf{i})_e & e \in D_s \\
(\mathbf{C}^T\boldsymbol{\nu}\mathbf{C}\mathbf{A})_e + i\omega(\boldsymbol{\sigma}_c\mathbf{A}_c + \boldsymbol{\sigma}_c\mathbf{G}_c\boldsymbol{\chi}_c)_e = 0 & e \in D_c \\
i\omega\left(\mathbf{G}_s^T\boldsymbol{\sigma}_s\mathbf{A}_s\right)_n + i\omega\left(\mathbf{G}_s^T\boldsymbol{\sigma}_s\mathbf{G}_s\boldsymbol{\chi}_s\right)_n = \left(\mathbf{G}_s^T\mathbf{i}\right)_n & n \in D_s \\
i\omega\left(\mathbf{G}_c^T\boldsymbol{\sigma}_c\mathbf{A}_c\right)_n + i\omega\left(\mathbf{G}_c^T\boldsymbol{\sigma}_c\mathbf{G}_c\boldsymbol{\chi}_c\right)_n = 0 & n \in D_c
\end{array} \tag{2}$$

where $\boldsymbol{\nu}$, $\boldsymbol{\sigma}_x$, $x \in \{s, c\}$, are the constitutive matrices, which can be considered as the discrete counterparts of the constitutive relations [4]. The subscripts s, c denote the subarrays or submatrices relative respectively to entities belonging to D_s or D_c. Moreover, we set $\mathbf{i} = \boldsymbol{\sigma}_s\mathbf{U}_s$.

The term $(\mathbf{G}_s^T\mathbf{i})_n, \forall n \in D_s$, assures that the continuity law is satisfied, therefore the ungauged A-χ formulation can be used [4]–[6] to solve (2).

Finally, the total current $I^j_{\rm tot}$ flowing in the jth active conductor can be easily determined in a post-processing stage as

$$I^j_{\rm tot} = -i\omega\mathbf{c}^{jT}\boldsymbol{\sigma}_s(\mathbf{A}_s + \mathbf{G}_s\boldsymbol{\chi}_s) + (\mathbf{c}^{jT}\boldsymbol{\sigma}_s\mathbf{c}^j)U^j_{\rm tot}. \tag{3}$$

[3]Thanks to the Poincaré–Lefschetz duality, $H^1(\mathcal{K}^j_s) \cong H_2(\mathcal{B}^j_s, \partial\mathcal{B}^j_s)$ holds [7]. Thus, the first cohomology group of $\mathcal{K}^j_s$ can be reinterpreted as the second relative homology group of the dual complex $\mathcal{B}^j_s$. The generator of this group consists of dual faces that form a surface S^j on dual complex having the boundary on $\partial\mathcal{K}^j_s$ and that is not itself boundary of any volume in $\mathcal{K}^j_s$.

IV. Localized Current Sources

In the A-χ geometric formulation, $I_{\rm tot}$ can only be specified using (3), which also gives a relationship between $I_{\rm tot}$ and $U_{\rm tot}$. The symmetric algebraic system of equations, having also $U_{\rm tot}$ as unknown, becomes

$$\begin{array}{ll}
(\mathbf{C}^T\boldsymbol{\nu}\mathbf{C}\mathbf{A})_e = 0 & e \in D_a \\
(\mathbf{C}^T\boldsymbol{\nu}\mathbf{C}\mathbf{A})_e + i\omega\boldsymbol{\sigma}_s(\mathbf{A}_s + \mathbf{G}_s\boldsymbol{\chi}_s)_e + (\mathbf{v})_e = 0 & e \in D_s \\
(\mathbf{C}^T\boldsymbol{\nu}\mathbf{C}\mathbf{A})_e + i\omega\boldsymbol{\sigma}_c(\mathbf{A}_c + \mathbf{G}_c\boldsymbol{\chi}_c)_e = 0 & e \in D_c \\
i\omega\left(\mathbf{G}_s^T\boldsymbol{\sigma}_s(\mathbf{A}_s + \mathbf{G}_s\boldsymbol{\chi}_s)\right)_n + (\mathbf{w})_n = 0 & n \in D_s \\
i\omega\left(\mathbf{G}_c^T\boldsymbol{\sigma}_c(\mathbf{A}_c + \mathbf{G}_c\boldsymbol{\chi}_c)\right)_n = 0 & n \in D_c, \\
-\mathbf{c}^{jT}\boldsymbol{\sigma}_s(\mathbf{A}_s + \mathbf{G}_s\boldsymbol{\chi}_s) + (\mathbf{c}^{jT}\boldsymbol{\sigma}_s\mathbf{c}^j)\frac{U^j_{\rm tot}}{i\omega} = \frac{I^j_{\rm tot}}{i\omega} & j = 1, \ldots, N
\end{array} \tag{4}$$

where $(\mathbf{v})_e = -\sum_{j=1}^{N}(\boldsymbol{\sigma}_s\mathbf{c}^j)_e U^j_{\rm tot}$ and $(\mathbf{w})_n = -\sum_{j=1}^{N}(\mathbf{G}_s^T\boldsymbol{\sigma}_s\mathbf{c}^j)_n U^j_{\rm tot}$.

The treatment of problems that require a combination of current and voltage sources follows easily by combining (2) and (4).

Furthermore, both the localized voltage sources and the localized current sources are easily generalized when a general external circuit is connected to the port of some active conductor. In this case, both $U_{\rm tot}$ and $I_{\rm tot}$ of that conductor have to be added as unknowns of (4). Correspondingly, an equation describing the external circuit has to be written into the linear system of (4).

V. Automatic Thick-Cut Computation

A. Previous Approaches

A general algorithm for the homology computations is well known since many decades ago [7], and it is based on the computation of the Smith Normal Form [7], [8]. This computation, although general, is quite time-consuming and cannot be naively applied even in the simplest practical problem. What is usually done is to apply some reduction algorithms that reduce the cardinality of the simplicial complex without changing its topology. The exploitation of the state-of-the-art reduction techniques like [9] is fundamental to have an implementation that can be used in practice [10], [11].

A couple of theoretical algorithms or implementations to compute the *thin cuts*—i.e., the representatives of the second relative homology group $H_2(\mathcal{K}^j_s, \partial\mathcal{K}^j_s)$ generators [11], [12]—have been proposed so far in [13] and [14]. Both approaches, due to the lack of efficient reduction techniques, result in a prohibitive computational time demonstrated by the absence of concrete results using real-sized meshes. Moreover, it is important to note that the direct thin cuts computation is in general not useful in practice for the thick-cuts computation. The reason is described in [11, Sec. 7.2.1].

There have been also some attempts to compute thin cuts using approaches based on homotopy [7]. These algorithms are born to compute the thin cuts in the complement of the conductive regions. Only the algorithms that construct a maximal acyclic subset M are relevant in case of cuts inside the conductors. The complement of M with respect to the torus-like region, in fact, might be a thin cut [15]–[18]. Other algorithms based on simple reduction technique [19] cannot be directly used in this context.

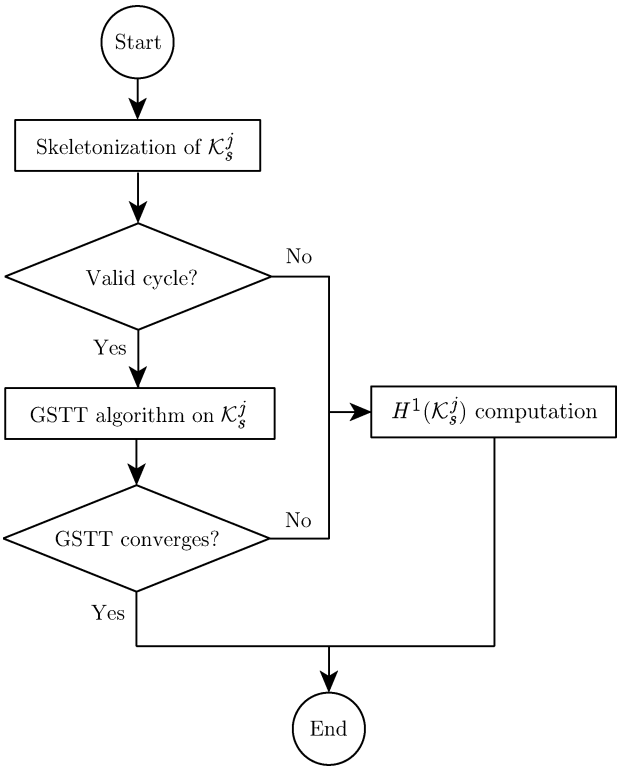

Fig. 2. Flowchart of the algorithm to find the thick cut.

The homotopical approach produces thin cuts that can be self-intersecting, which again is a problem for thick-cut extraction, as pointed out in [11, Sec. 7.2.1]. In fact, all homotopical methods do not get the coefficients of the thick cuts, so a post-processing (possibly very hard in general) to get coefficients of the thick cut is needed. Moreover, in most practical cases, these algorithms produce additional dangling surfaces, which have to be eliminated in some way; see, for example, the *filtering* in [18].

B. Proposed Algorithm

The presented algorithm works for each $\mathcal{K}_s^j, j = \{1, \ldots, N\}$ separately.

The idea is to use an approach based on *skeletonization* and *Generalized Spanning Tree Technique* (GSTT) [11], [20], which is very fast and works on most cases, but it may fail for some input. In case of problems, which are extremely rare in practice, there is the theoretical guarantee to detect them and resort to the computation of the first cohomology group generators with state-of-the-art reduction techniques, which is more computationally expensive but general.

The flowchart of the proposed algorithm is illustrated in Fig. 2. The description of each step of the flowchart will be given in this section.

1) Data Structures Used in the Algorithm: The simplex data structure is assumed to posses the following fields:

1) an integer value `dimension`, pointing the dimension of the simplex;
2) a boolean flag `deleted`, initially imposed to `false`;
3) sets of pointers to boundary (`bd`) and coboundary (`cbd`) elements of the simplex [8].

The `deleted` flag is used to mark the simplices deleted during the skeletonization procedure without physically removing them from the data structure.

2) Skeletonization: The skeletonization procedure has been developed as an attempt to mimic the mathematical concept of retraction [7]. The procedure presented below, based on a *free face*[4] *collapsation* [8], aims in reducing a three-dimensional conductor into one-dimensional graph being its homotopy retract. The simplex F is denoted as *free face* if it is a face of exactly one nondeleted simplex C. As demonstrated in [8], the simplices $\{F, C\}$ can be deleted from the complex without changing its homology and homotopy type.

The skeletonization algorithm works on the list L consisting of all free faces in the complex. At the beginning of the algorithm, all the free faces in the initial complex $\mathcal{K}$ are added to the list L. Then, until L is nonempty, in each iteration of the *while* loop, a simplex F is taken out of L.

If F is still a face of exactly one element C such that $C.deleted =$ `false`, then it is set $F.deleted := C.deleted :=$ `true`. Then, each of the nondeleted boundary elements of C that is a free face is added to the list L.

If F has no nondeleted elements in the coboundary anymore (what can happen once the element in the coboundary of F was reduced with its other free face), then each of the boundary elements of F that is a free face is added to the list L.

It can be demonstrated that once the size of the boundary and coboundary of each simplex are uniformly bounded by a constant, then the complexity of the presented procedure is linear with respect to the number of simplices in the complex. The output of the algorithm, referred to as a *skeleton* of the complex $\mathcal{K}_s^j$, consists of all the nondeleted simplices. In most practical problems, the skeleton will consists of zero- and one-dimensional simplices only.

3) Validation of the Skeleton: The GSTT algorithm [11]–[20] requires as an input, when dealing with a torus-like region, a cycle that has to be connected, not self-intersecting, and has to "go 1 time around the conductor, inside it."[5] In order to test the skeleton obtained by the skeletonization algorithm, one has to check if all the two- and three-dimensional simplices in $\mathcal{K}_s^j$ are deleted. If so, the skeleton is a valid input for the GSTT. The validation procedure is linear with respect to the number of all simplices in the simplicial complex.

4) Generalized Spanning Tree Technique (GSTT): In order to obtain the thick cut from a valid skeleton of $\mathcal{K}_s^j$, the GSTT algorithm is used on the initial complex $\mathcal{K}_s^j$. A detailed description of the algorithm can be found in [11, Sec. 8.3]. It can be demonstrated that the algorithm complexity is linear with respect to the number of elements in the simplicial complex. However, in some uncommon situations, it may happen that the GSTT algorithm does not converge. In this marginal case, to have a general procedure, a pure computation of the first cohomology group over integers is used.

5) First Cohomology Group Computations: For the computations of the first cohomology group generator of the complex $\mathcal{K}_s^j$, a modified version of [10] code is used. Before the pure

[4]By a face of a d-dimensional simplex S, we refer to any of its $(d-1)$-dimensional subsimplices; see [8].

[5]It is worth to note that not all homology generators $H_1(\mathcal{K}_s^j)$ fulfill all these requirements. In particular, with automatic homology computations, it is quite likely for such a generator to be not connected and/or self-intersecting.

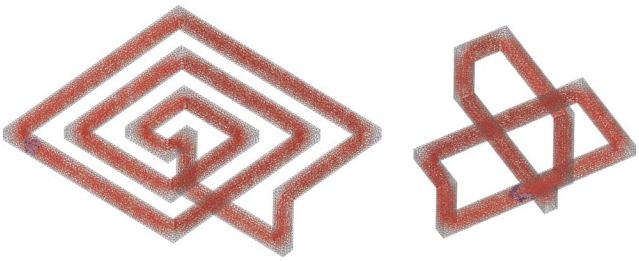

Fig. 3. (left) Current density in a planar inductor. (right) Current density in a knotted torus.

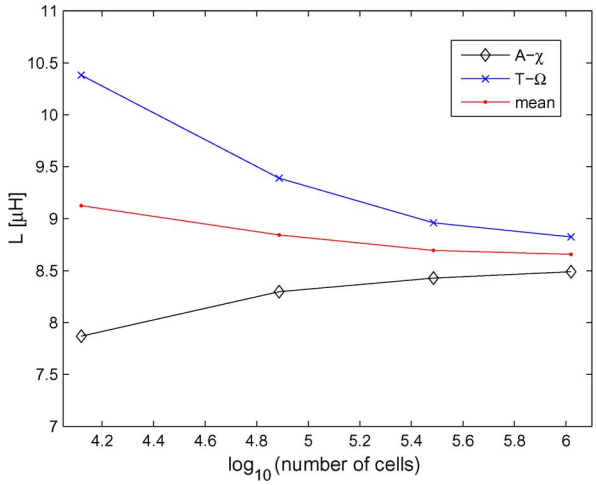

Fig. 4. Convergence of the planar inductor inductance with mesh refinement using both A-χ and T-Ω complementary eddy-current formulations. The meshes employed in the two formulations are the same.

Smith Normal Form computations, the [9] reduction technique is used, which makes the computations much more efficient.

The complexity of the cohomology computation may be far bigger with respect to the complexity of the previous approach based on skeletonization and GSTT. However, it should be noted that the cases when pure topological computations are needed are very rare in practice, as will be shown in Section VI. Moreover, efficient reduction techniques employed make the cohomology computation much faster with respect to the worst-case analysis regarding the pure Smith Normal Form computation.

VI. Numerical Results

The localized voltage and current source approach was tested on many examples of massive conductors. For example, on the left of Fig. 3, the resulting current density in a planar inductor is shown. On the right of Fig. 4, another example consisting in a knotted torus is presented.

The convergence of the inductance of the coil on the left of Fig. 3 with respect to the mesh refinement is shown in Fig. 4. The results obtained by the A-χ formulation are compared to the ones obtained by the complementary T-Ω geometric formulation [11] on the same mesh showing a very good agreement.

In all the tested examples, the skeletonization algorithm returned a valid skeleton, and the GSTT always converged. For each example, many different randomly generated trees were used without experiencing any problem. The trees used are *minimal diameter trees* that are easily constructed using *Breadth-first strategy* (BFS) [21].

Acknowledgment

This work was supported in part by Polish Grant MNiSzW nr N201 037 31/3151.

References

[1] A. Bossavit, "How weak is the weak solution in finite elements methods?," *IEEE Trans. Magn.*, vol. 34, no. 5, pp. 2429–2432, Sep. 1998.

[2] T. Weiland, "A discretization method for the solution of Maxwell's equations for six-component fields," *Electron. Commun. (AEÜ)*, vol. 31, no. 3, p. 116, 1977.

[3] E. Tonti, "Algebraic topology and computational electromagnetism," in *Proc. 4th Int. Workshop Electr. Magn. Fields*, Marseille, France, May 12–15, 1988, pp. 284–294.

[4] R. Specogna and F. Trevisan, "Discrete constitutive equations in $A-\chi$ geometric eddy-currents formulation," *IEEE Trans. Magn.*, vol. 41, no. 4, pp. 1259–1263, Apr. 2005.

[5] P. Dular, F. Henrotte, and W. Legros, "A general and natural method to define circuit relations associated with magnetic vector potential formulations," *IEEE Trans. Magn.*, vol. 35, no. 3, pt. 1, pp. 1630–1633, May 1999.

[6] R. Specogna and F. Trevisan, "Voltage sources with $A-\chi$ discrete geometric approach to eddy-currents," *Eur. Phys. J.—Appl. Phys.*, vol. 33, pp. 97–101, 2006.

[7] J. R. Munkres, *Elements of Algebraic Topology*. Cambridge, MA: Perseus, 1984.

[8] T. Kaczynski, K. Mischaikow, and M. Mrozek, *Computational Homology*. Berlin, Germany: Springer-Verlag, 2004, vol. 157, Applied Mathematical Sciences.

[9] T. Kaczynski, M. Mrozek, and M. Slusarek, "Homology computation by reduction of chain complexes," *Comput. Math.*, vol. 35, no. 4, pp. 59–70, 1998.

[10] "The CAPD library" [Online]. Available: capd.wsb-nlu.edu.pl

[11] P. Dłotko, R. Specogna, and F. Trevisan, "Automatic generation of cuts on large-sized meshes for the $T-\Omega$ geometric eddy-current formulation," *Comput. Methods Appl. Mech. Eng.*, vol. 198, pp. 3765–3781, 2009.

[12] P. R. Kotiuga, "On making cuts for magnetic scalar potentials in multiply connected regions," *J. Appl. Phys.*, vol. 61, no. 8, pp. 3916–3918, 1987.

[13] P. W. Gross and P. R. Kotiuga, *Electromagnetic Theory and Computation: A Topological Approach*. Cambridge, U.K.: Cambridge Univ. Press, 2004, vol. 48.

[14] S. Suuriniemi, "Homological computations in electromagnetic modeling," Ph.D. dissertation, Tampere University of Technology, Tampere, Finland, 2004, 952-15-1237-7.

[15] Z. Ren, "T-Ω formulation for eddy-current problems in multiply connected regions," *IEEE Trans. Magn.*, vol. 38, no. 2, pt. 1, pp. 557–560, Mar. 2002.

[16] J. Simkin, S. C. Taylor, and E. X. Xu, "An efficient algorithm for cutting multiply connected regions," *IEEE Trans. Magn.*, vol. 40, no. 2, pt. 2, pp. 707–709, Mar. 2004.

[17] P. Dular, "Curl-conform source fields in finite element formulations: Automatic construction of a reduced form," *COMPEL—Int. J. Comput. Math. Electr. Electron. Eng.*, vol. 24, no. 2, pp. 364–373, 2005.

[18] A. T. Phung, O. Chadebec, P. Labie, Y. Le Floch, and G. Meunier, "Automatic cuts for magnetic scalar potential formulations," *IEEE Trans. Magn.*, vol. 41, no. 5, pp. 1668–1671, May 2005.

[19] P. J. Leonard, H. C. Lai, R. J. Hill-Cottingham, and D. Rodger, "Automatic implementation of cuts in multiply connected magnetic scalar region for 3-D eddy current models," *IEEE Trans. Magn.*, vol. 29, no. 2, pp. 1368–1371, Mar. 1993.

[20] A. Bossavit, *Computational Electromagnetism*. New York: Academic, 1998.

[21] T. H. Cormen, C. E. Leiserson, R. L. Rivest, and C. Stein, *Introduction to Algorithms*, 2nd ed. Cambridge, MA: MIT Press, 2001.